Bulletin of Geosciences, Vol. 79, No. 1, 41–52, 2004
© Czech Geological Survey, ISSN 1214-1119

The lithology, geochemistry, and metamorphic gradation of the crystalline basement of the Cheb (Eger) Tertiary Basin, Saxothuringian Unit

Jiří Fiala – Zdeněk Vejnar

Academy of Sciences of the Czech Republic, Institute of Geology, Rozvojová 135, 165 00 Praha 6, Czech Republic. E-mail: fiala@gli.cas.cz

Abstract. The crystalline basement of the Cheb Tertiary Basin is comprised of muscovite granite of the Smrčiny Pluton and crystalline schists of the Saxothuringian Unit. With increasing depth (as seen from the 1190 m deep drill hole HV-18) this crystalline schist exhibits rapid metamorphic gradation, with the characteristic development of garnet, staurolite, and andalusite zones of subhorizontal arrangement. The dynamic MP-MT and static LP-MT crystallization phases were followed by local retrograde metamorphism. The moderately dipping to subhorizontal S_2 foliation, which predominates in the homogeneous segments, is followed by subvertical S_3 cleavage.

The vertical succession of psammo-pelitic, carbonitic, and volcanogenic rock sequences, together with geochemical data from the metabasites, indicates a rock complex representing an extensional, passive continental margin setting, which probably originated in the Late Cambrian to Early Ordovician. On the contrary, the geochemistry of the silicic igneous rocks and of the limestone non-carbonate components point to the compressional setting of a continental island arc. This disparity can be partly explained by the inheritance of geochemical characteristics from Late Proterozoic rocks in the source region.

Key words: crystalline basement, Cheb Tertiary Basin, Saxothuringian, lithology, geochemistry, metamorphism

Introduction

The Cheb Tertiary Basin is considered to be a westernmost member of the Tertiary basin system of the Krušné hory (Erzgebirge) piedmont in NW Bohemia. The marked W–E dip of the basin bottom (ca 0–300 m), and the eastern limitation on the Mariánské Lázně fault line, make them similar to the Tertiary relics of the Cheb-Domažlice half-graben (Vejnar, Zoubek et al. 1962, Tomas and Vejnar 1965). The Miocene, Pliocene, and ± Oligocene sediments are largely composed of fluvial and lacustrine clays, sands, and gravels, with local intercalations of coal clays and seams of low-quality brown coal (Šantrůček 1957, 1980).

The basin sediments are interrupted by numerous faults, which are mostly of synsedimentary type. According to earlier interpretations, this fault system led to the origin of an asymmetric, step-like, unilateral graben trending NNW–SSE (Čepek in Zoubek et al. 1963). According to a later study (Václ 1979), two orthogonal and two diagonal fault systems led to the parquet-like arrangement of minor blocks.

The basement of the basin includes Saxothuringian crystalline schists and granitoids of the Smrčiny Pluton. The boundaries of both units (Vejnar 1960, Forman and Obr 1977) are well known (Fig. 1) from the results of extensive drilling connected to hydrogeological studies of the Františkovy Lázně area (Václ 1979, Pazdera 1980).

The basement of the northern part of the basin (area of Plesná – Nový Kostel) is comprised of muscovite-biotite schists, and by local garnet-bearing mica-schists that also outcrop in the vicinity of the basin. These rocks are usually lithostratigraphically ranked to the Late Proterozoic and Cambrian (Škvor and Sattran 1974), and to the Middle and Late Cambrian (Emmert et al. 1981, Hoth et al. 1995), respectively. Further to the south the basin basement is formed by two-mica and muscovite granites from the younger intrusive phase of the Smrčiny Pluton (Vejnar 1960). The remaining southern part of the basin basement is mainly composed of metapelites and metapsammites,

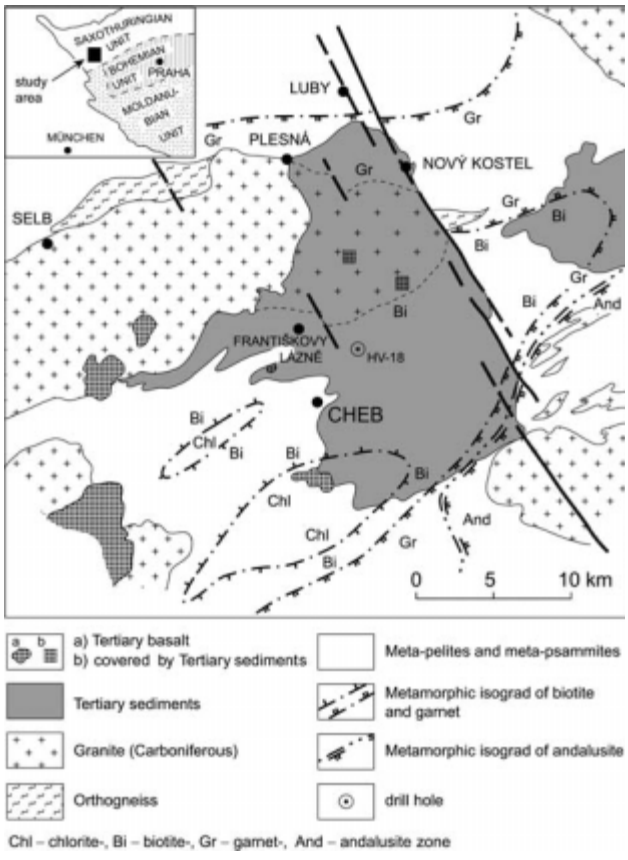

Figure 1. The crystalline basement of the Cheb Tertiary Basin and its surroundings.

the mineral parageneses of which correspond to muscovite-biotite schists (muscovite + biotite + albite An 8–10), though they resemble phyllites in appearance. Along the SW basin rim the basement consists of chlorite-sericite phyllite, while a small segment of the SE rim is also comprised of mica-schists with garnet and staurolite or andalusite (see Fig. 1).

The lithostratigraphic ranking of crystalline schists in the southern part of the basin basement has complicated the age interpretations of the corresponding rocks cropping out in the basin surroundings. To the SW these rocks are mostly considered to be Ordovician (Emmert et al. 1981, Fiala and Vejnar 1997); to the NE, however, they are ranked as Late Proterozoic (Emmert et al. 1981) to Cambrian (Škvor and Sattran 1974), or to various sequences of the Early and Middle Cambrian (Hoth et al. 1995). These problems remain unsolved due to the lack of robust lithological or lithogeochemical criteria. The petrographic character of the crystalline schists of the basin floor points only to metamorphosed psammo-pelitic sediments, probably of Ordovician and partly (in the northern basin segment) of Cambrian age (Phycode and Warmensteinach formations).

Relations of the basin crystalline basement schists to the metamorphic structure of the surrounding units

The drill holes that have been bored into the basement have encountered mostly muscovite-biotite mica-schists (Pazdera 1980), which contain sporadic garnet only in the northern part. This observation correlates with the courses of biotite and garnet isograds of the adjacent exposed areas (see Fig. 1). The delimited isograds and chlorite zone segments, situated W and SW of Cheb, form a symmetric NE–SW oriented ellipsoidal structure of regional metamorphism, with its axis plunging to the SE. In the central part of this structure rocks of the chlorite zone are juxtaposed against rocks containing garnet, staurolite, and andalusite.

This homogeneous complex of crystalline schists is surrounded by Variscan granitoids of the Karlovy Vary and Smrčiny plutons, and by granitoids of the northern part of the Oberpfalz area. The contacts with granite intrusions are very steep in the given area, which shows the small extent of the contact aureole of the Srmčiny Pluton W of Cheb. This was also observed in the superdeep KTB drill hole in the vicinity of the granite outcrops (e. g., Emmermann, 1995). Thus, the idea that the metasedimentary complex forms only a thin sheet on top of the granite basement (Emmert et al. 1981) does not seem plausible. The present authors instead believe this metasedimentary complex to be deeply rooted.

Lithology

The consideration of drill core data suggests that the basement of the basin forms a lithologically uniform crystalline complex. Besides the muscovite and two-mica granites of the Smrčiny Pluton, the metamorphosed pelitic and psammo-pelitic sediments with sandy layers of mm- to dm-thicknesses were the most frequently encountered rock types. However, as is shown by the HV-18 drill core, the depth-dependent variability of the basement crystalline complex is conspicuous (at least at that site).

Within the profile of this nearly 1200 m deep drill hole three markedly different lithological sequences appear in the basement below the Tertiary sediments (Fig. 2). Ascending from the bottom of the drill core, the depth from 1190 to 590 m is comprised of the volcano-sedimentary sequence, followed by the carbonate sequence to a depth 450 m, while the rest of the section up to the level of the basin bottom at 237 m is comprised of the uniform psammo-pelitic sequence. The individual sequences pass continuously into each other, without any boundaries indicative of a lithostratigraphic hiatus.

The lower part of the volcano-sedimentary sequence consists of a variegated complex of metamorphosed psammo-pelitic rocks with numerous 0.1–2 m thick metabasite layers and minor intercalations of micaceous quartzite, locally containing carbonate, rarely with polymetallic and pyritic mineralization. Volcanic activity of the WPB type (Vejnar 1991a) is evidenced at a depth of around 750 m by the deposition of four 4–7 m thick metabasite layers. On top of these rests the ca 40 m thick horizon of metamorphosed psammo-pelitic rocks with mute-ball texture, separating the metabasites from the overlying ca 25 m thick layer of silicic metavolcanics. The latter are feldspar-rich and markedly oriented, containing two micas and up to 3 mm porphyritic microcline and plagioclase with compositions from An 15 to 20. The above-mentioned mute-balls, the sizes of which are on the order of mm to cm, are composed of a fine mosaic of quartz with some micas and plagioclase, rarely accompanied by K-feldspar. The chemical similarity between the mute-ball rocks and silicic metavolcanics (cf. Table 2) suggests that the mute-balls represent disintegrated layers of the original silicic ash-tuffs deposited at the beginning of the felsic volcanic activity. The section of the volcano-sedimentary sequence terminates with the deposition of several thin metabasite layers.

The carbonate-bearing sequence starts with a complex of rapidly alternating layers of locally graphite-bearing carbonate schist, with layers of sandy limestone and black shales. This sequence, which is finely banded upwards at its base, gradually becomes coarser. In the course of the upward increase in sedimentary differentiation, the rock maturity culminates within the depth of around 490–500 m with the deposition of two 4–6 m thick, whitish limestone banks separated by a black shale layer about 7 m thick. The sequence terminates rapidly above these carbonate banks, and at a depth around 450 m passes into the uniform sequence of metapelites and metapsammites. Analogous sequences have been found in the broader basin surroundings, and are generally ranked to the Lower Ordovician (Frauenbach and Phycode formations).

The search for fossils in the above mentioned rocks, which would lead to their stratigraphic ranking, was unsuc-

cessful. Though they cannot be well identified, radiolaria remnants have been observed in the black shales (Dr. Konzalová, Geological Institute of Academy of Sciences of the Czech Republic, Prague, pers. com.). The samples studied by Dr. Prössl of the University of Giessen (pers. com.) show that all of the organic remnants represent fine, unidentifiable detritus that probably originated from microorganism activity during sedimentation.

Geochemical data (Table 1) show the relatively high purity of the crystalline limestones, with a minimum of dolomite-component. This is markedly different than the carbonate rocks that form the well known layer at the Saxothuringian/Moldanubian boundary near Vysoká (Vejnar 1991b). Geochemical data from the metabasites point to basaltic effusions and tuffs of the WPB type (Vejnar 1991a).

The vertical sequence and facies development of the rocks encountered in drill core HV-18, together with lithogeochemical data of the metabasites, point to a rock complex of the contourite type, originating along a passive continental margin. The occurrence of bimodal volcanic centers, accompanied locally by limestones and black shales, is characteristic of such geotectonic settings.

Metamorphic evolution and its variability with depth

The extent of individual metamorphic zones in the surroundings of the Cheb basin (see Fig. 1), namely the zones of biotite and chlorite, points to relatively flat, regional metamorphic zoning. The results of drilling exploration in the broader surroundings, such as in the area of Dyleň (Vejnar 1991b), also suggest such an arrangement. The analysis of the region's metapelite and metapsammite mineral parageneses leads to the consideration of polymetamorphic evolution encompassing three phases (Gaertner and Schmitz 1968, Vejnar 1991b, Fiala and Vejnar 1997). The dynamic phase is characterized by the syntectonic crystallization of mica, garnet, and staurolite, while the post-deformational, mostly static, phase mainly produced andalusite. The final regressive phase is characterized by sericitization and chloritization.

The influence of the granite intrusions on the regional-metamorphic structure is weak. A biotite hornfels zone only a few tens of metres thick is present at the contact with the porphyric granite of the Smrčiny Pluton. In the segments where the pluton forms two-mica and muscovite granite, hornfels pass into a zone of secondary muscovitization (the Františkovy Lázně surroundings).

The variability of metamorphic evolution with depth is shown by the ca 1190 m deep HV-18 drill hole situated about 5 km NE of Cheb (see Fig. 1). Such metamorphic variability was found mainly in the psammo-pelitic lithologies, i. e. the mica-schists. Their meso-structural fabrics and mineral parageneses are identical to those of analogous rocks from the Cheb-Dyleň Unit. Relics of the primary sedimentary structures are best preserved in mica-schists with mute-ball textures. In these rocks the original fine-sandy

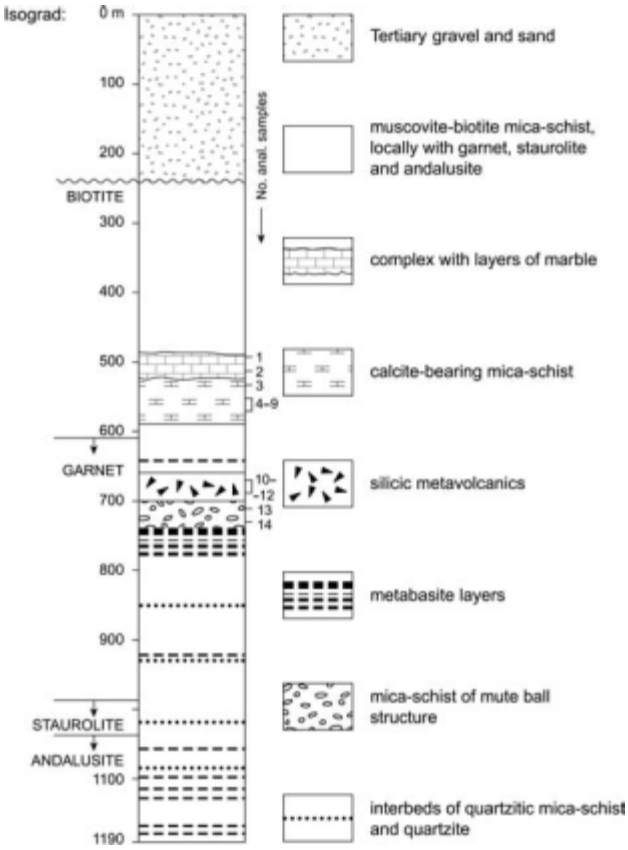

Figure 2. Profile of the HV-18 borehole, Cheb Tertiary Basin.

mute-balls are markedly deformed along the S_1 and S_2 planes, and locally stretched into folds which show an S_3 axial-plane cleavage.

As is shown by the drill cores, the character of the main S_2 foliation is highly variable. This foliation is markedly planar, with moderate to subhorizontal dips in homogeneous to weakly banded segments. In finely banded mica-schists this foliation is intensely folded, and its dip fluctuates up to a subvertical S_3-parallel orientation. In spite of these local structural fluctuations, we believe that a more or less original lithostratigraphic sequence is preserved within the whole drill section. This interpretation is also consistent with the observed sequence of the primary lithological variability.

The mineral parageneses determined from the HV-18 drill core confirms the analogous tectonometamorphic evolution with rocks of the Cheb-Dyleň Unit. Three metamorphic-crystallization phases were delimited as follows:

1. Syntectonic prograde phase with characteristic mineral parageneses:
   muscovite I + biotite I
   muscovite I + biotite I + garnet
   muscovite I + biotite I + garnet + staurolite
2. Post-tectonic (locally late tectonic) prograde phase with parageneses:
   biotite II + muscovite II
   biotite II + muscovite II + andalusite
3. Retrograde phase with parageneses:
   chlorite + sericite ± calcite, epidote, pyrite, sphalerite.

The distribution of the above mentioned mineral parageneses within the drill profile led to the demarcation of three metamorphic crystallisation phases: the first phase encompassing the biotite, garnet, and staurolite zones; the second phase accounting for the andalusite zone; while the third retrograde phase affected the crystalline schists of the whole drill profile. This last phase was especially intense within the biotite zone, where the extensive chloritization and sericitization of earlier minerals caused the phyllitic appearance of the mica-schists. The third phase was followed by the formation of minor carbonate or quartz veins locally containing pyrite, vermiculite, and rarely also galena and sphalerite. The influence of this phase was extreme within numerous, mostly subvertical, fault zones, the filling of which corresponds to so-called diaphtorite II of Schreyer (1965) from the adjacent Bavarian area.

The fine- to small-grained mica-schists in the biotite zone become coarser in the deeper metamorphic zones, with increasing proportions of biotite and garnet, or staurolite and andalusite, respectively. The basic nature of the plagioclase (An 8 – An 12) increases simultaneously, as do the occurrences of quartz secretions with local plagioclase.

The biotite of the mica-schists is deep brown in colour, but gains a reddish tint within deeper zones. In micaceous sections biotite, often accompanied by ilmenite, forms 1 to 5 mm idioblasts, oriented partly across to the main S_2 foliation. Locally poikilitic biotite contains quartz and garnet inclusions, and passes into the form corresponding to biotite II. The latter appears mostly in the vicinity of andalusite poikiloblasts as their complementary crystallization component.

Garnet (1–3 mm) appears as skeletal crystals, some of which are deformed into S-form. They often show a disintegrated texture, and are cemented with quartz. Minute garnet grains (ca 0.5 mm) often arranged in chains following the fold structure of the rock, appear in the quartz-rich mica-schist bands. Garnet grains up to 5 mm in diametre are macroscopically observable within the lower part of the garnet zone and in the andalusite zone; they are idioblastic, with obvious traces of zoned textures in the crystal rims. Preliminary analyses of the larger idioblasts show a prograde compositional zoning of between 60 and 70 % almandine and 25 to 15 % spessartite.

Staurolite (0.3–1 mm) is present mainly within mica-rich bands of garnet- and andalusite-bearing mica-schists. It shows the characteristic marks of mechanical deformation, pointing to syntectonic crystallization.

Andalusite (0.5–15 mm) usually grows along metamorphic foliation planes into the mica-rich matrix of the mica-schists. It metasomatically penetrates the matrix, the remnants of which were gradually spent or became enclosed. Thus originate poikiloblasts which are densely filled with quartz, biotite I, garnet, and staurolite inclusions. They are often plate-shaped and partly limited by the foliation planes. The older fold structure, marked by scales of biotite I and platy ilmenite, remains fully preserved in the andalusite poikiloblasts. The sequence of the first and second crystallization phases of the mica-schists is thus well documented.

Geochemistry

From the HV-18 drill cores mostly rocks of the carbonate sequences (Table 1) and silicic magmatic rocks (Table 2) were selected for geochemical studies. In both cases the samples were correlated with their potential equivalents in the Saxothuringian Unit from the broader surroundings of the HV-18 site.

Metamorphosed carbonate-bearing rocks

The geochemical data for the metamorphosed carbonate-bearing rocks from the HV-18 drill core are listed in Table 1. Brief characterizations of the individual samples are as follows:

Sample No.	Depth	Rock
1/928	489 m	Whitish fine-grained marble with individual bluish bands.
2/916	501 m	White small-grained marble with graphitic mica-schist laminae.
3/910	515 m	Gray muscovite-biotite calcitic mica-schist with graphitoid pigment.
4/929	535 m	Gray, muscovite-biotite, calcitic mica-schist with graphitoid pigment and isolated gray fine-grained marble laminae.
5/926	545 m	Similar to previous sample.
6/920	558 m	Gray, muscovite-biotite, calcitic mica-schist with graphitic mica-schist laminae.
7/918	570 m	Markedly banded gray, muscovite-bio-
8/911	578 m	tite, calcitic mica-schist, with alterna-
9/927	582 m	ting bands of carbonate or graphitoid composition.

The geochemistry of the HV-18 carbonate-bearing rocks in Table 1 was compared with the analyses of Wiegand (1996) for metacarbonates of the Arzberg Unit from Wunsiedel. The results of this comparison define a series from nearly pure calcite marble up to calcitic mica-schist with substantial amounts of detritic components. As the majority of the minor and trace elements are included within the non-carbonate components, the carbonate fraction was subtracted using the determined CO_2 contents. The corrected data thus approximate the geochemistry of the detritic components of the metacarbonates.

A comparison of the compositions of individual non-carbonate components shows some inverse proportionality between the detritus content and its minor and trace element enrichments. In the detritus of the purer carbonates the pelite component seems to dominate, preferentially concentrating most of the minor and trace elements.

The geochemistry of the non-carbonate component is shown as a spider-diagram in Fig. 3, where the average compositions for the HV-18 and Wunsiedel samples are plotted in normalized form (norm = composition of primitive mantle according Taylor and McLennan 1985). For comparison, the normalized composition of the upper

Table 1. Geochemistry of carbonate-bearing rocks

Rock	crystalline limestone		calcitic mica-schist, locally with graphite and marble or mica-schist laminae						
Locality	HV-18	HV-18	HV-18	HV-18	HV-18	HV-18	HV-18	HV-18	HV-18
Sample No.	1/928	2/916	3/910	4/929	5/926	6/920	7/918	8/911	9/927
SiO_2 [%]	3.11	3.86	51.67	55.89	59.19	54.25	58.42	15.58	55.59
TIO_2	0.05	0.07	0.68	0.83	0.76	0.63	0.65	0.26	0.60
Al_2O_3	1.05	1.46	14.33	15.46	15.49	14.41	12.88	7.63	12.41
FeO_{tot}	0.35	0.42	4.62	5.62	4.96	4.73	4.02	2.87	3.19
MnO	0.22	0.11	0.58	1.33	0.58	0.42	0.61	1.33	0.50
MgO	0.76	0.68	3.36	2.86	2.74	3.09	1.92	1.34	1.78
CaO	51.94	51.29	12.66	7.44	6.34	10.20	8.99	39.16	11.33
Na_2O	0.20	0.20	0.90	2.51	2.30	1.31	2.01	1.00	1.60
K_2O	0.15	0.19	2.85	2.18	2.71	3.58	3.01	0.77	3.02
P_2O_5	0.07	0.04	0.17	0.24	0.26	0.24	0.15	0.10	0.19
CO_2	40.64	39.90	5.24	3.48	3.16	4.47	5.26	28.98	7.87
H_2O^+	0.59	0.87	2.01	2.59	1.33	1.94	1.80	1.03	1.58
H_2O^-	0.12	0.39	0.37	0.25	0.20	0.52	0.47	0.42	0.17
Sum	99.25	99.48	99.44	100.68	100.02	99.79	100.19	100.47	99.83
Cs [ppm]	0.5	0.5	7.5	3.3	6.1	4.7	3.9	1.8	2.6
Rb	11	14	166	109	54	138	95	22	92
Ba	17	18	980	562	1095	1649	1000	342	890
Pb	21	25	23	21	31	20	25	19	29
Sr	278	171	221	508	278	340	266	434	348
Y	0.5	1	27	33	36	31	28	8	28
Th	0.5	1.4	10.3	9.7	5.3	9.8	10.3	4.7	10.8
U	0.5	0.5	3.2	3.7	3.8	4.1	5.8	0.5	3.7
Zr	15	7	141	192	302	174	220	54	255
Hf	0.5	0.5	4.7	5.3	6	4.7	6.1	1.5	6.1
Sn	3	2	4	7	7	8	6	3	5
Nb	0.5	0.5	6	12	8	9	12	1	8
Ta	0.5	0.5	0.5	0.5	0.5	1.2	0.5	0.5	0.5
Ga	0.5	0.5	6	9	9	8	6	0.5	4
Cu	0.5	0.5	14	3	20	19	10	0.5	23
Co	1.2	1.1	12.7	15.9	11.9	12.5	10.7	6.2	8.6
Ni	5	6	20	37	26	21	21	14	18
Sc	1	1.3	13.3	12.7	11.9	12.9	10.4	6.2	9.2
V	21	21	54	62	67	62	46	36	47
Cr	0.5	0.5	38	50	38	40	32	0.5	23
Zn	0.5	0.5	43	19	44	37	28	0.5	19
La	4.06	5.03	36.8	39.9	40.4	37.2	35.4	9.46	38.1
Ce	7.26	7.33	69.3	73.8	73.9	72.2	69.6	15.5	68.4
Sm	0.5	0.5	6.75	7.46	7.73	6.47	6.37	1.93	6.74
Eu	0.13	0.15	1.15	1.29	1.33	1.21	1.18	0.39	1.14
Tb	0.1	0.1	0.1	1.01	1	1.02	1.06	0.1	0.1
Yb	0.5	0.5	2.81	2.45	1.67	3.78	3.1	1.56	2.89
Lu	0.05	0.05	0.49	0.55	0.22	0.28	0.47	0.25	0.4

continental crust (UCC) is also plotted. Relative to UCC, a marked enrichment in almost all elements is observed in the non-carbonate components. This is evidently connected to the increased sedimentary maturity of this material relative to the average UCC composition. Differences is sediment maturity are also evident between the HV-18 and Wunsiedel samples. Thus, the element enrichment is higher in the Wunsiedel averages than in those of HV-18, because of the prevalence of purer carbonates in the former, and of impure carbonates in the latter.

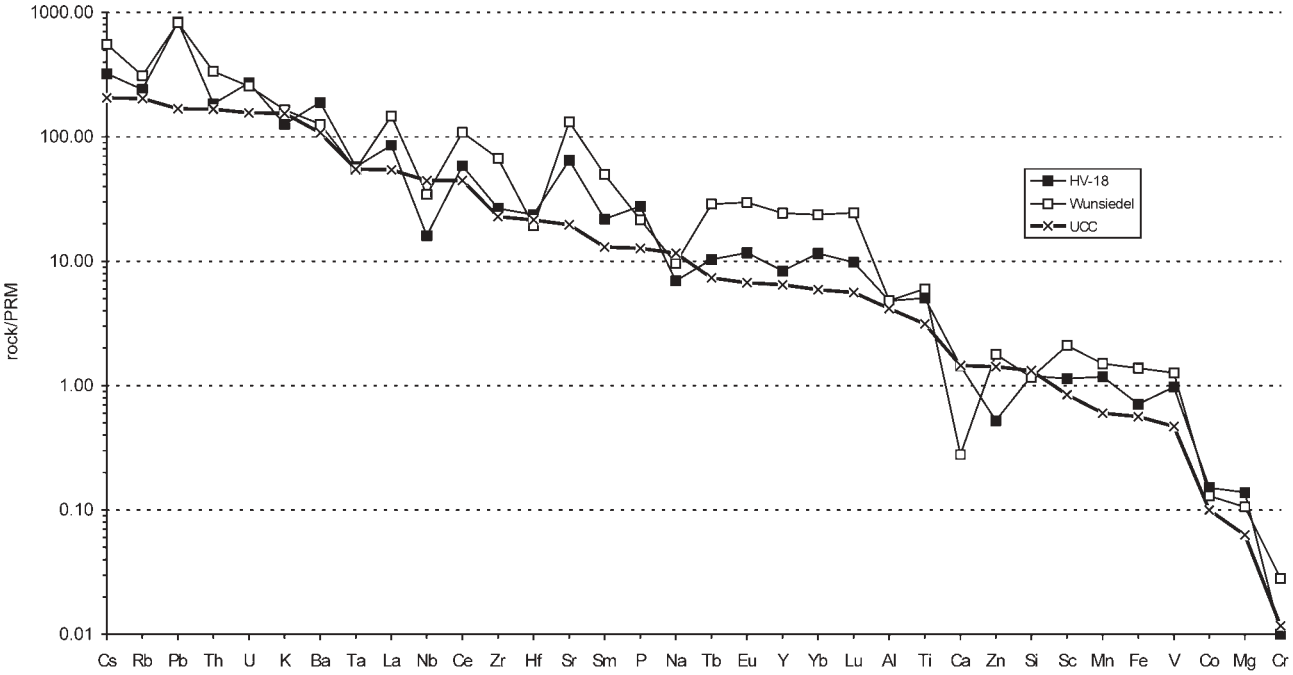

Figure 3. Geochemistry of detritic components of metacarbonates.

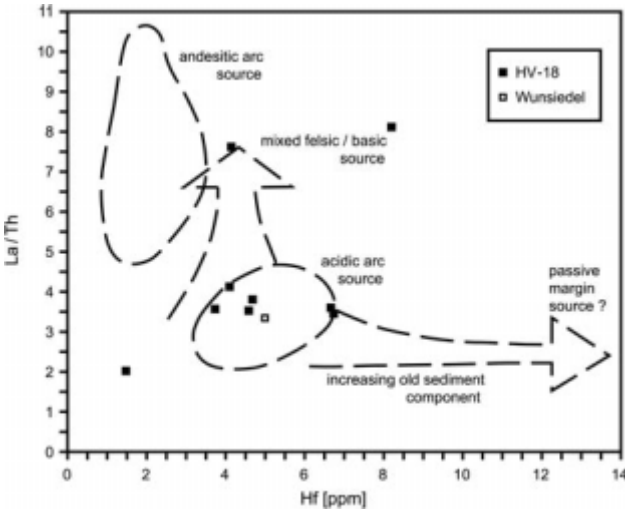

Figure 4. Metacabronate detritus in the plot of Floyd and Leveridge (1987).

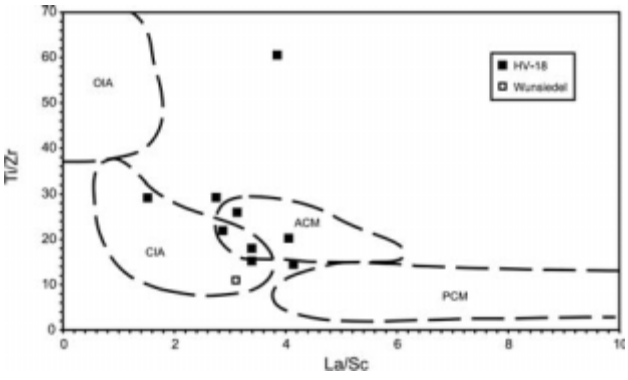

Figure 5. Metacarbonate detritus in the La/Sc vs Ti/Cr plot of Bhatia and Crook (1986).

The perfect correlation between some elemental contents in the Wunsiedel and HV-18 samples, as seen in Fig. 3, may point to co-genetic relations in their geotectonic settings and probably also their ages of deposition. The observed negative Nb anomaly is usually interpreted as an indication of orogenic settings in the sediment source region (e.g., Bonjour and Dabard 1991). The negative Ca anomaly of the Wunsiedel sample probably reflects a correction error in the carbonate content.

The geochemical characteristics of sediments can supply information about the geotectonic settings of their origin. Projections based on major element variations (e.g., Bhatia 1983) were excluded because of the possibility that their concentrations have undergone changes. Projections based on less mobile trace elements such as La, Th, Hf, Zr, Ti, Sc, and Co were considered to be more suitable. In the Hf vs. La/Th diagram of Floyd and Leveridge (1987) (Fig. 4) the non-carbonate components plot in the "acidic arc source" field, i. e. magmatic arc settings on a continental basement with predominantly silicic magmatism. The projections of Bhatia and Crook (1986) lead to similar conclusions: an orthogonal La/Sc vs. Ti/Zr (Fig. 5), and triangular Th-Co-Zr/10 (Fig. 6) and Th-Sc-Zr/10 (not shown) diagrams show the non-carbonate components generally plotting in the continental island arc (CIA) field.

The Sr-isotopic study of the HV-18 metacarbonates (Wiegand 1996) supplied an isochron at 495 ±12 Ma and $Sr_i = 0.7087 \pm 1$. These data are interpreted as the probable age of sedimentation of the carbonate sequences at the Cambrian/Ordovician boundary.

Silicic igneous rocks

In the drill cores of HV-18 the silicic igneous rocks are represented by rocks that were probably deposited originally as rhyolite tuffs. The mica-schists with mute-ball textures also contain high amounts of silicic volcanic material,

and probably originated as layers of ash-tuffs disintegrated by slumping processes. The silicic igneous rocks of HV-18 rocks are geochemically characterized in Table 2, where they are complemented by data from orthogneiss outcrops near Kaceřov at the E border of the Cheb Basin. Briefly, the characteristics of analyzed samples are as follows:

Sample No.	HV-18	Rock
10/932	667 m	Light grey, locally whitish, homogeneous, small-grained silicic metavolcanic rock (German term "epigneis"), probably of rhyolitic or rhyolitic-tuff character.
11/930	690 m	
12/934	695 m	Similar to above samples, hints of the mute-ball texture appear at the base.
13/923	710 m	Dark-gray, small-scaly muscovite-biotite mica-schists with numerous very fine quartz-feldspar mute-balls of mm- to cm-size, and with isolated lens-like laminae of basic and silicic metavolcanics.
14/913	717 m	
Fi-23	Kaceřov	Rocky outcrop, partially broken off above the dam lake 4.5 km N of Kaceřov. Markedly foliated, silver-white, small-grained muscovite orthogneiss with minor biotite.
Fi-24	Kaceřov	Abandoned quarry above the dam lake 4.5 km N of Kaceřov. Medium-grained muscovite orthogneiss with feldspar porphyro-clasts up to 5 mm, and minor biotite.

Various metamorphosed silicic igneous rocks from adjacent areas of Fichtelgebirge, SE Germany were selected for comparison: silicic orthogneisses of Wunsiedel, Waldershof and Selb, and the so-called "epigneis" rocks, which are probably silicic metavolcanics. Comparative data in the individual diagrams given below utilize the arithmetic means obtained from the analyses of Wiegand (1996) and of Siebel at al. (1997). The data from these sources may be listed as follows: Wiegand – Wunsiedel (2 analyses), Waldershof (1 analysis) and "Epigneis" (1 analysis); Siebel at al. – Wunsiedel (11 analyses), Waldershof (13 analyses), Selb (6 analyses), and "Epigneis" (W-complex 14 analyses, E-complex 10 analyses and S-complex 10 analyses).

The content of the detrital sedimentary component within the mica-schists with mute-ball textures was evaluated using the AN–AL–Q triangular projection (Fig. 7) from Weisbrod (1970), which simulates the ratios among feldspar (AN), mica (AL), and quartz (Q) components, and is therefore suitable for differentiating between ortho- and para-rocks. In this diagram the above mentioned mica-schists plot within para-field, yet close to the curve separating both fields. These rocks were thus considered to be suitable for further correlation. The silicic metavolcanics (HV-18, "Epigneis" rocks) and the Kaceřov orthogneisses exhibit similar positions, which is probably caused by considerable secondary alterations such as the muscovitization and silicification of these rocks. Such processes are accompanied by strong depletion of Na, Ca, and Sr, and enrichment in Si, K, and Ba (cf. Siebel et al. 1997). In the Weisbrod diagram the final effect of these chemical changes results in the movement of individual plots away from the AN corner [AN = K + Na + Ca; AL = Al + Fe_{tot} + Mg-(K + Na + 2Ca); Q = Si-2(Na + Ca) in atomic ratios recalculated to 100%].

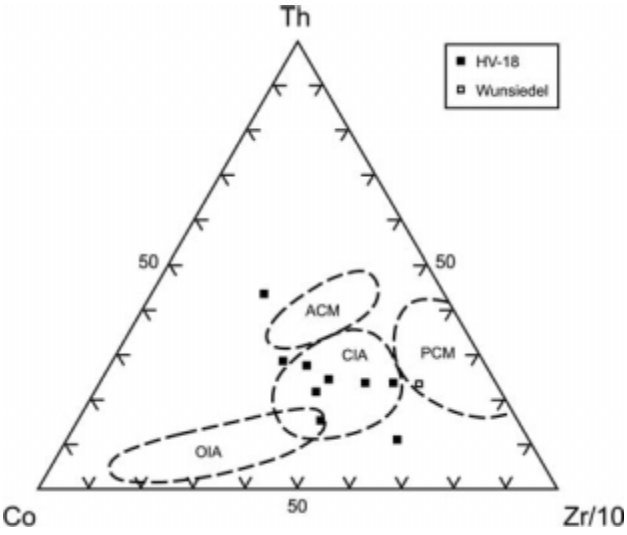

Figure 6. Metacarbonate detritus in the Co-Zr/10-Th plot of Bhatia and Crook (1986).

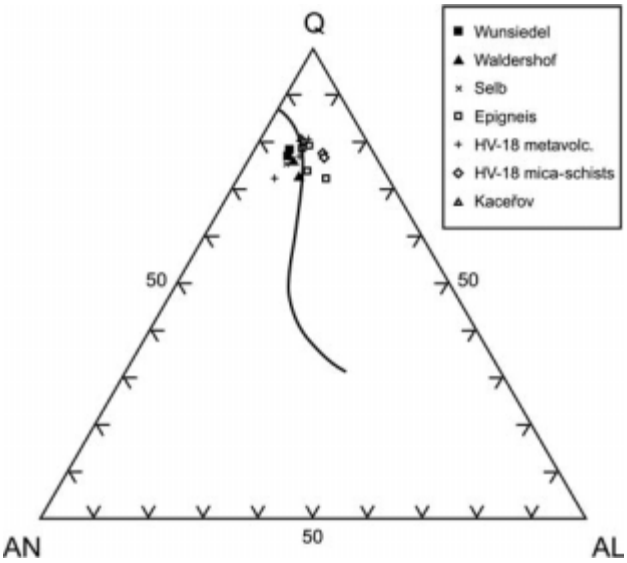

Figure 7. Silicic igneous rocks in the plot Weisbrod (1970).

To avoid the influence of low-grade metamorphism and alterations, the compositions of the original igneous rocks were determined using plots for less mobile elements, such as Zr, Ti, Y, Nb, Ta, and Yb. For the classification of the metamorphosed silicic magmatic rocks the Nb/Y vs Zr/TiO_2 plot of Winchester and Floyd (1977) was preferred (Fig. 8). All orthogneisses and metavolcanics in this diagram fall almost exclusively within the rhyodacite–dacite field, which is in agreement with the results obtained on analogous material by Siebel et al. (1997). In the following paragraphs we describe how the

Table 2. Geochemistry of silicic igneous rocks

Rock	silicic metavolcanics			mica-schist mute-ball		orthogneiss	
Locality	HV-18	HV-18	HV-18	HV-18	HV-18	Kaceřov	Kaceřov
Sampl. No.	10/932	11/930	12/934	13/923	14/913	Fi-23	Fi-24
SiO_2 [%]	72.11	69.83	75.46	73.11	74.02	77.68	76.83
TiO_2	0.33	0.55	0.20	0.69	0.70	0.11	0.10
Al_2O_3	14.04	14.71	13.03	13.14	12.71	12.48	13.26
FeO_{tot}	2.35	3.07	1.71	3.86	3.56	0.95	0.93
MnO	0.32	0.39	0.27	0.70	0.27	0.00	0.10
MgO	0.65	0.59	0.39	0.89	0.78	0.23	0.22
CaO	1.42	2.00	0.99	0.96	0.54	0.22	0.13
Na_2O	1.90	4.01	1.70	1.51	1.81	2.97	1.90
K_2O	4.82	3.61	4.20	3.58	3.44	3.00	5.17
P_2O_5	0.26	0.47	0.09	0.20	0.12	0.14	0.09
H_2O^+	1.05	0.67	0.79	1.20	1.07	0.90	0.91
H_2O^-	0.16	0.15	0.2	0.45	0.33	0.12	0.27
Sum	99.41	100.05	99.03	100.29	99.35	98.80	99.91
Cs [ppm]	7	7.4	3.2	7.4	7.6	2.98	5.11
Rb	204	190	184	174	130	151	217
Ba	705	678	690	618	597	349	406
Pb	33	30	39	20	22	34	16
Sr	153	204	181	85	100	26.4	27
Y	48	48	44	41	39	20	17
Th	12.4	11.9	10	19.2	18.6	7.37	6.63
U	7.2	7	7.4	7.6	3.6	4.54	5.4
Zr	194	160	101	486	433	108	129
Hf	6.5	3.3	4	14.3	11.4	2.42	2.46
Sn	12	8	11	8	8	19	19
Nb	6	6	9	11	12	5	5
Ta	1	1	1	1	1	1	1.09
Ga	10	9	10	8	9	14	13
Cu		10		17	4	5	6
Co	4.3	6.8	1.3	9.8	9.7	0.5	0.434
Ni	9	12	1	14	14	2.5	2.5
Sc	6	8.7	4.5	9.3	9.1	5	5.06
V	27	37	24	46	40	10	10
Cr	1	13		25	23	3.8	3.98
Zn	9	18	9	24	25	30.7	30.2
La	24	30.2	15.7	44.8	41.5	9.28	9.25
Ce	46.5	60.3	35.1	86.2	88.8	18.67	18.66
Nd						9.51	8.81
Sm	6.09	7.21	4.45	8.38	7.79	2.5	2.41
Eu	0.87	1.33	0.31	1.47	1.39	0.231	0.21
Gd						3	2.35
Tb	1.04	1.21	0.5	1.01	1.3	0.522	0.507
Ho						0.884	0.898
Tm						0.35	0.367
Yb	3.97	3.98	4	3.81	4.63	2.49	2.36
Lu	0.65	0.46	0.52	0.5	0.59	0.354	0.314

various discriminative diagrams were used to determine the possible geotectonic settings of the magma origin.

The diagram of Ti/Nb vs SiO_2 (Bonjour and Dabard 1991) should distinguish between orogenic (mostly compressional) and anorogenic (mostly extensional) geotectonic settings for magma origins. In this graph (Fig. 9) the entire sample group plots as a consistent trend situated far in the field of orogenic magmas.

The set of diagrams by Pearce et al. (1984) enables the further division of orogenic magmas into syn-collisional (syn-COLG) and volcanic arc (VAG) granites, and of anorogenic magmas into intraplate (WPG) and ocean-ridge (ORG) granites. All of these projections used: Y + Nb vs Rb (Fig. 10), Yb vs Ta (Fig. 11), Yb + Ta vs Rb, and Y vs Nb (the latter two not shown here). The silicic igneous rocks sampled for this study define a homogeneous group situated within the orogenic magma region in the VAG field or at the VAG/syn-COLG boundary. A similar conclusion has been obtained by Wiegand (1996).

The chondrite-normalized REE-distribution patterns of silicic orthogneisses are documented in Fig. 12. Individual distribution curves represent arithmetic means of the data from Wunsiedel (5 analyses), Waldershof (3 analyses), and Selb (2 analyses), as published by Wiegand (1996), Siebel et al. (1997), and Kaceřov (2 analyses, in the present paper). All of these exhibit a moderate descent within the succession of light rare earth elements (LREE), and a nearby sub-horizontal course within the heavy rare earths (HREE). From Waldershof towards Kaceřov the distribution patterns gradually decrease in bulk REE content (157–47 ppm) and La/Yb ratio (5.7–2.6), and increase in negative europium anomalies Eu/Eu* (0.44–0.26). According Siebel et al. (1997), such trends are a typical attribute of the progressing differentiation of peraluminous S-type granites. Based on this interpretation, the Waldershof orthogneiss is less differentiated and thus more closely approaches the composition of the primary magma, while the Kaceřov orthogneiss, on the contrary, represents a highly evolved differentiate. The arrow in Fig. 12 thus indicates the evolutionary trend caused by fractional crystallization. In general, the depletion of REE is attributed to the removal of accessory phases. The LREE are esspecially susceptible to removal by such phases as allanite and monazite. The Eu depletion is ascribed to the removal of plagioclase and alkali feldspar during differentiation (cf. Siebel et al. 1997).

The REE distribution patterns of the metavolcanic rocks are shown in Fig. 13, where the arithmetic means of 4 “epigneis” rock analyses from Wiegand (1996) and Siebel et al. (1997) serve for comparison. An enveloping orthogneiss data set from Fig. 12 is also plotted. One can see that the distribution curves of the metavolcanics accumulate in the vicinity of the upper boundary of the orthogneiss envelope, i. e. in the area of the less-differentiated magmas. If we suppose co-genetic relations for the plutonic and volcanic rocks of this study, it may lead to the consideration of the more direct derivation of volcanic magmas from the source region, without pronounced differentiation in a magmatic chamber.

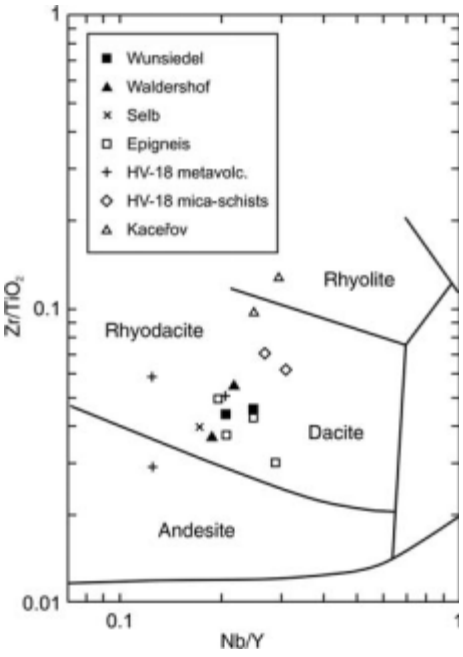

Figure 8. Silicic magmatic rocks in the Zr/TiO_2 vs. Nb/Y plot of Wichester and Floyd (1977).

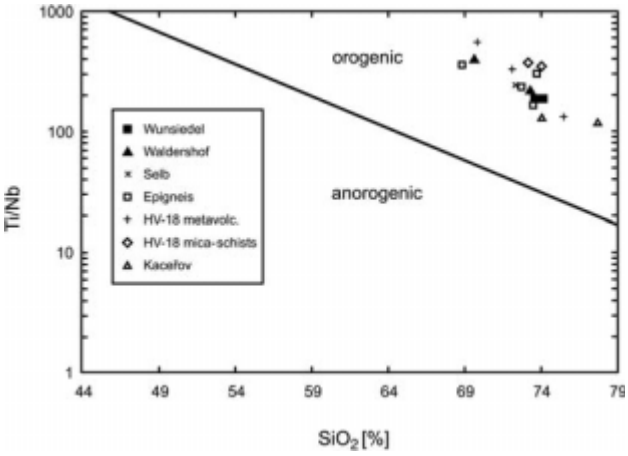

Figure 9. Silicic igneous rocks in the SiO_2 vs. Ti/Nb plot of Bonjour and Dabard (1991).

Several of the silicic igneous rocks we studied have been radiometrically dated using U-Pb from zircon (Wiegand 1996), and Rb-Sr (Wiegand 1996, Siebel et al. 1997) and Sm-Nd whole-rock methods (Siebel et al. 1997). The U-Pb zircon method on the Wunsiedel orthogneiss yields a minimum intrusion age of 455 ± 8 Ma, while the Rb-Sr method gave isochrons at 466 ± 8 Ma (Wiegand 1996) and 480 ± 4 Ma (Siebel et al. 1997). Zircon from the similar orthogneiss of Waldershof was analyzed by the U-Pb method, with the result of 458 ± 4 Ma as the minimum intrusion age. The complex Sm-Nd isochron for the Wunsiedel, Waldershof, and Selb orthogneisses gives an age of 560 ± 45 Ma (Siebel et al. 1997).

In interpreting the U-Pb data, it must be considered that the ages were determined from only two or three zircon populations. As other populations yield gradually lower ages, it is possible that the whole U-Pb system suffered ra-

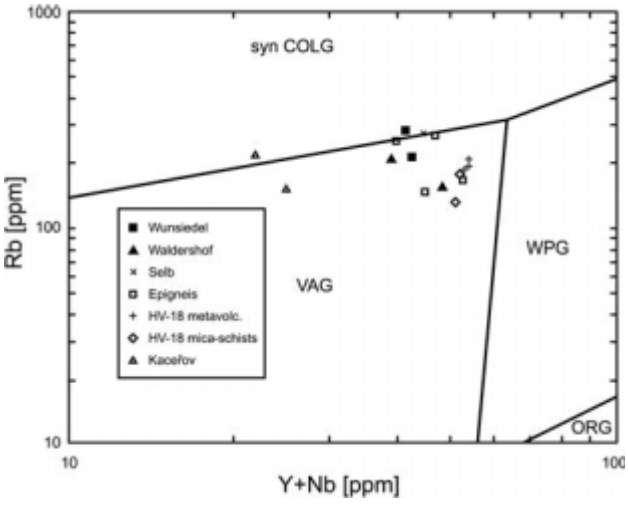

Figure 10. Silicic igneous rocks in the Y + Nb vs. Rb plot of Pearce et al. (1984).

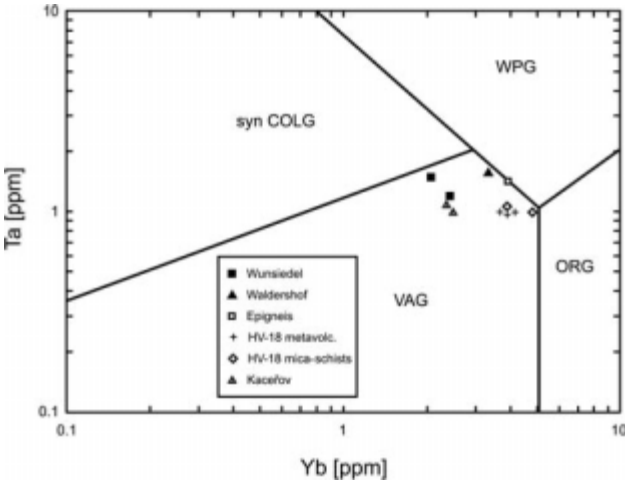

Figure 11. Silicic igneous rocks in the Yb vs. Ta plot of Pearce et al. (1984).

diogenic lead loss, and that the actual intrusion ages are older. This is also suggested by the considerably earlier Rb-Sr ages (up to 480 Ma) and the much older Sm-Nd ages. In less altered systems the relation between the data sets is just the opposite. In the Central Bohemian Pluton, for example, the Rb-Sr age of the Blatná granodiorite was found to be 331 ± 4 Ma (van Breemen et al. 1982), while an age of 346 ± 10 Ma was obtained using the U-Pb zircon evaporation method (Holub et al. 1997). From this analogy the minimum intrusion age of the orthogneisses mentioned above should be at least 480–495 Ma. The minimum intrusion age of 443 ± 13 Ma was determined from the silicic metavolcanic rock (epigneis) from Wernersreuth (Wiegand 1996). At another locality (NW Fichtelgebirge) this value has been constrained at 449 ± 4 Ma (Teufel 1988). In both cases the actual extrusion age must be much higher with regard to the sedimentation age of the surrounding Phycode Formation. As the age of this formation has been constrained to the Tremadocian (the base of the Arenig, Falk et al. 1995), the actual extrusion age of the metavolcanics should also lie within the time span of 480–495 Ma (according to latest time-table of Haq and van Eysinga 1998).

The geochemistry of HV-18 metabasites (Vejnar 1991a) ranks their original magmas as sub-alkalic tholeites. They are enriched in incompatible and light rare earth elements, and correspond to the tholeiites of oceanic islands or of rifts on attenuated continental crust. Metabasites of very similar geochemistry and inferred geotectonic settings were described by Kachlík (1993) from the Kladská Unit, which is usually interpreted as a part of the Saxothuringian Unit overthrusted by rocks of the Mariánské Lázně Complex.

In the segment of Saxothuringian Unit that has been studied so far, the geotectonic settings of magmatism and sedimentation are usually interpreted as being connected with Early Paleozoic crustal extension (Falk et al. 1995). Both the character of the sedimentation and the geochemistry of the basic members of the bimodal magmatism are consistent with this interpretation. On the contrary, the geochemistry of the silicic magmatic rocks and the non-carbonate components of the limestones point to the orogenic setting of a continental island arc. The idea that the silicic igneous and non-carbonate components inherited geochemical characteristics from a source region that had been built up from a Late Proterozoic volcano-sedimentary complex in a continental island arc setting is one possible explanation for this disparity (cf. Dörr et al. 1998, Fiala et al. 1995).

Conclusions

The crystalline basement of the Cheb Tertiary Basin is built up of the muscovite granite of the Smrčiny Pluton and the Saxothuringian crystalline schists. These schists comprise the base of Tertiary sediments represented by muscovite-biotite mica-schists of phyllitic appearance. With increasing depth (as seen from drill core HV-18) these crystalline schists exhibit rapid metamorphic gradation with the characteristic development of garnet, staurolite, and andalusite zones. The index mineral isograd extends into the basin surroundings. This suggests a sub-horizontal arrangement of individual metamorphic zones and, thus, of paleo-isotherms with rapid depth gradation.

The analysis of the mineral parageneses of the crystalline schists suggests two prograde phases and one retrograde phase. The first prograde phase is represented by the syn-deformational crystallization of garnet and staurolite under conditions between low- and medium-pressure metamorphism. The second prograde phase is represented by the formation of andalusite, and bears the marks of thermally static, low-pressure crystallization. The third, retrograde, phase led to the decomposition of the above mentioned mineral phases, entailing reactions such as chloritization, sericitization, and carbonatization.

S_2 foliation of variable orientation predominates in the crystalline schists of the HV-18 drill core. This foliation is markedly planar, with moderate to subhorizontal dips in

its homogeneous segments. This foliation is intensely folded in the finely-banded mica-schists, while its dip fluctuates widely up to subvertical S_3-cleavage parallel orientations.

The vertical succession and facies evolution of the psammo-pelitic, carbonitic, and volcanogenic rock sequences, together with the geochemical character of the metabasites, seem to indicate a rock complex of contourite type. This complex is likely to have originated during the Late Cambrian to Early Ordovician, along a passive continental margin with characteristic occurrences of local, bimodal volcanic centers and of basins with sediment fillings of carbonaceous and black shales. On the contrary, the geochemistry of the silicic igneous and the non-carbonate components of the limestone point to the orogenic settings of a continental island arc. This can be partly explained by the inheritance of geochemical characteristics from Late Proterozoic rocks of the source region.

Acknowledgements. We thank G. Zulauf and the official reviewers V. Žáček and V. Kachlík for their constructive reviews and assistence with English. Financial support from the Grant Agency of the Czech Republic (grant 205/99/0907) is gratefully acknowledged.

References

Bhatia M. R. (1983): Plate tectonics and geochemical composition of sandstones. J. Geol. 91, 611–627.

Bhatia M. R., Crook K. A. W. (1986): Trace element characteristics of graywackes and tectonic setting discrimination of sedimentary basins. Contrib. Mineral. Petrology 92, 181–193.

Bonjour J.-L., Dabard M.-P. (1991): Ti-Nb ratios of clastic terrigeneous sediments used as an indicator of provenance. Chem. Geol. 91, 257–267.

Breemen van O., Aftalion M., Bowes D. R., Dudek A., Mísař Z., Povondra P., Vrána S. (1982): Geochronological studies of the Bohemian massif, Czechoslovakia, and their significance in the evolution of Central Europe. Trans. Roy. Soc. Edinbburgh, Earth Sci. 73, 89–108.

Dörr W., Fiala J., Vejnar Z., Zulauf G. (1998): U-Pb Zircon ages and structural development of metagranitoids of the Teplá crystalline complex: evidence for pervasive Cambrian plutonism within the Bohemian Massif (Czech Republic). Geol. Rundsch. 87, 135–149.

Emmert U., von Horstig G., Stettner G. (1981): Geologische Übersichtkarte 1 : 200 000 CC6334 Bayreuth. BGR, Hannover.

Emmermann R. (1995): Abendteuer Tiefbohrung. Eine Zwischenbilanz zum Abschluß des Kontinentalen Tiefbohrprogramms der Bundesrepublik Deutschland (KTB). Geowissenschaften 13, 114–128.

Falk F., Franke W., Kurze M. (1995): V. B Autochthon and nonmetamorphic nappe units. V.B.1 Stratigraphy. In: Dallmeyer R. D., Franke W., Weber K. (eds) Pre-Permian geology of Central and Eastern Europe. Springer, Heidelberg, 221–234.

Fiala J., Henjes-Kunst F., Müller-Sigmund H., Vejnar Z. (1995): The prograde metamorphic series of the Teplá Crystalline Complex and the Zone of Erbendorf-Vohenstrauß – a geochemical and Sr-Nd isotopic comparison. Terra Nostra 95/8, 94.

Fiala J., Vejnar Z. (1997): The Cheb-Dyleň crystalline unit, relations to the Moldanubian Zone. J. Geol. Sci., Geol. 47, 56–57.

Floyd P. A., Leveridge B. E. (1987): Tectonic environment of the Devonian Gramscatho basin, south Cornwall: framework mode and geochemical evidence from turbiditic sandstones. J. Geol. Soc. (London) 144, 531–542.

Forman J., Obr F. (1977): Příspěvek k poznání podloží sokolovské a chebské pánve. Sbor. geol. Věd, Geol. 29, 103–115.

Gaertner von H. R., Schmitz H. H. (1968): Geologisch-petrographische Beobachtungen in der Grenzzone Moldanubikum/Saxothuringikum in der nördlichen Oberpfalz. Geol. Jb. 85, 315–370.

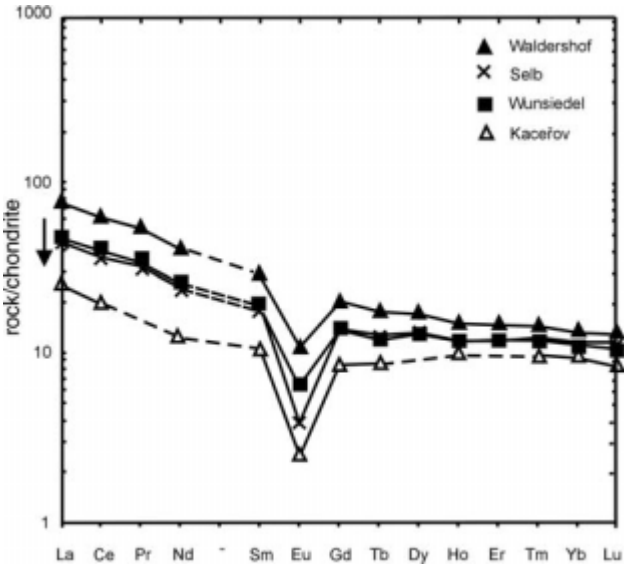

Figure 12. Normalised REE distribution of orthogneiss rocks.

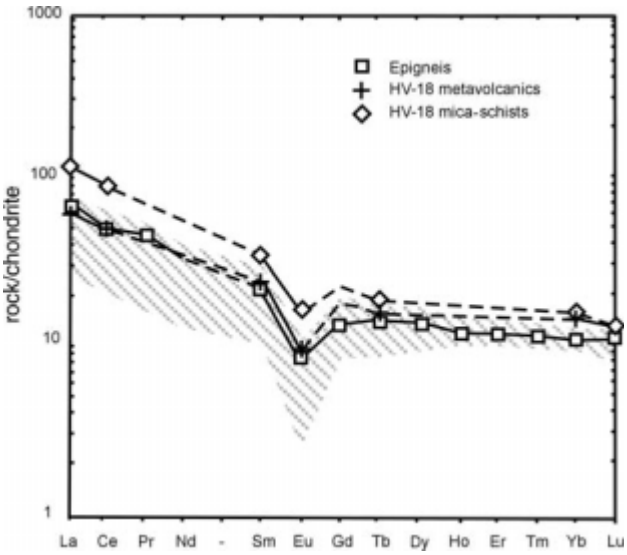

Figure 13. Normalised REE distribution of metavolcanic rocks.

Haq B. U., van Eysinga F. W. B. (1998): Gelogical time table. Elsevier, Amsterdam.

Holub F. V., Cocherie A., Rossi P. (1997): Radiometric dating of granitic rocks from the Central Bohemian Plutonic Complex (Czech Republic): constraints on the chronology of thermal and tectonic events along the Moldanubian-Barrandian boundary. C. R. Acad. Sci. Paris 325, 19–26.

Hoth K., Wasternack H., Berger J., Breiter K., Mlčoch B., Schovánek P. (1995): Geologische Karte Erzgebirge/Vogtland 1 : 100 000. Freiberg.

Kachlík V. (1993): The evidence for Late Variscan nappe thrusting of the Mariánské Lázně Complex over the Saxothuringian terrane (West Bohemia). J. Czech Geol. Soc. 38, 1–2, 43–58.

Pazdera A. (1980): Závěrečná zpráva Odravská pánev – hydrogeologie. Report, Geofond, Praha.

Pearce J. A., Harris N. B. W., Tindle A. G. (1984): Trace element discrimination diagrams for the tectonic interpretation of granitic rocks. J. Petrol. 25, 956–983,

Schreyer W. (1965): Metamorpher Übergang Saxothuringikum-Moldanubikum östlich Tirschenreuth/Opf. nachgewiesen durch phasenpetrologische Analyse. Geol. Rundsch. 55, 491–509.

Siebel W., Raschka H., Irber W., Kreuzer H., Lenz K.-L., Höhndorf A., Wendt I. (1997): Early Paleozoic Acid Magmatism in the Saxo-

thuringian Belt: New insights from a geochemical and isotopic study of orthogneisses and metavolcanic rocks from the Fichtelgebirge, SE Germany. J. Petrol. 38, 2, 203–230.

Šantrůček P. (1957): Stratigraficko-litologické poměry s. části chebské pánve. Čas. Mineral. Geol. 2, 411–422.

Šantrůček P. (1980): Geologická stavba a výrony minerálních vod s CO_2 v chebské a sokolovské pánvi. In: Mahel M. (ed.) Vážnejšie problémy geologického vývoja a stavby Československa. Geol. Úst. D. Štúra., Bratislava, 207–228.

Škvor V., Sattran V. (1974): Krušné hory západní část, soubor oblastních geologických map 1 : 50 000. Ústřední ústav geologický, Praha.

Taylor S. R., McLennan S. M. (1985): The continental crust: its composition and evolution. Blackwell, Oxford.

Teufel S. (1988): Vergleichende U-Pb- und Rb-Sr-Altersbestimmungen an Gesteinen des Übergangsbereiches Saxothuringikum/Moldanubikum, NE-Bayern. Göttinger Arbeiten zur Geologie und Paläontologie 35, 1–87.

Tomas J., Vejnar Z. (1965): Terciérní relikty jižní části chebsko-domažlického příkopu. Věst. Ústř. Úst. geol. 40, 3, 153–158.

Václ J. (1979): Geologická stavba chebské pánve a jejího okolí. Geol. Průzk. 21,133–135.

Vejnar Z. (1960): Der tschechoslowakische Teil des fichtelgebirgischen Granitmassivs. Sbor. Ústř. Úst. geol 26, odd. geol., 217–285.

Vejnar Z. (1991a): Metabasites from the drill hole Cheb HV18, West Bohemian Saxothuringian region. Věst. Ústř. Úst. geol. 66, 4, 201–213.

Vejnar Z. (1991b): Structural and metamorphic patterns of the calc-silicate and metapelitic rocks from Vysoká, western Bohemia, and remarks on the Saxothuringicum/Moldanubicum boundary. Věst. Ústř. Úst. geol. 66, 6, 349–364.

Vejnar Z., Zoubek V. et al. (1962): Vysvětlivky k přehledné geologické mapě ČSSR 1 : 200 000 Mariánské Lázně – Švarcava. Ústřední ústav geologický, Praha.

Weisbrod A. (1970): Pétrologie du socle métamorphique des Cévenes médianes (Massif Central français). Reconstitution sédimentologique et approche thermodynamique du métamorphisme. Thèse d'état, Nancy, 3 Vols.

Wiegand B. (1996): Isotopengeologische und geochemische Untersuchungen zur prävariskischen magmatischen und sedimentären Entwicklung im saxothuringisch-moldanubischen Übergangsbereich (Grenzgebiet BRD/CR). Dissertation Theses, Universität Göttingen.

Winchester J. A., Floyd P. A. (1977): Geochemical discrimination of different magma series and their differentiation products using immobile elements. Chem. Geol. 20, 325–343.

Zoubek V., Hoth K., Lorenz W. et al. (1963): Vysvětlivky k přehledné geologické mapě ČSSR 1 : 200 000 Karlovy Vary – Plauen. Ústřední ústav geologický, Praha.